

HOW TO MITIGATE THE DISTRIBUTION SHIFT PROBLEM IN ROBOTICS CONTROL: A ROBUST AND ADAPTIVE APPROACH BASED ON OFFLINE TO ONLINE IMITATION LEARNING

Anonymous authors

Paper under double-blind review

ABSTRACT

Distribution shift in imitation learning refers to the problem that the agent cannot plan proper actions for a state that has not been visited during the training. This problem can be largely attributed to the inherently narrow state-action coverage provided by expert demonstrations over the full environment. In this paper, we propose a robust offline to adaptive online imitation learning framework that handles the distribution shift problem in a lifelong, multi-phase scheme. In the offline learning phase, we leverage supplementary demonstrations to broaden the state-action coverage of the policy by utilizing a discriminator to effectively train the policy with supplementary demonstrations, thereby enhancing the robustness of the policy to distribution shift. In the subsequent online inference phase, our framework detects the occurrence of distribution shift and conducts self-supervised imitation learning from online experiences to adapt the policy to the online environments. Through extensive evaluations in MuJoCo environments, we demonstrate that our method exhibits better robustness to distribution shift and better adaptation performance to online environments than the baseline algorithms, which indicates superior performance of our framework against the distribution shift.

1 INTRODUCTION

Recently, a variety of learning-based approaches such as imitation learning (IL) and reinforcement learning (RL) have achieved notable success in various robotics control tasks (Fu et al., 2024; Choi & Seo, 2025). However, these methods suffer from the distribution shift problem (Yoon et al., 2024), where the robot fails to act appropriately when encountering novel states during the online inference phase that were not present in the offline training dataset. In general, the state-action coverage of expert demonstrations spans only a narrow subset of the entire environment's state-action space, making IL especially vulnerable to distribution shift (Mehta et al., 2025; Panaganti et al., 2023). To address this, several studies have been proposed that focus on mitigating distribution shift in the offline training phase (Mehta et al., 2025; Ke et al., 2023), or in the online inference phase (Gong et al., 2024; Ho & Ermon, 2016). However, both approaches still exhibit several limitations.

For the offline phase, previous research (Mehta et al., 2025; Laskey et al., 2017a; Ke et al., 2023) aim to make the policy robust to distribution shift via dataset augmentation techniques. Laskey et al. (Laskey et al., 2017a) proposed to collect expert demonstrations in which a human intentionally encounters and recovers from various perturbation scenarios. However, this approach requires the human expert to provide demonstrations across a wide range of situations and perturbations, which is highly costly in practice. An alternative method (Ke et al., 2023) involves learning a world model from expert demonstrations and then performing data augmentation by generating a virtual dataset through rollouts of the learned model. This approach can expand the state-action coverage of the offline dataset, however, its performance is vulnerable to the modeling error (Yu et al., 2020). For the online phase, previous research (Gong et al., 2024; Ho & Ermon, 2016) focus on adapting the policy to the online environment by leveraging the agent’s online experiences. Gong et al. (Gong et al., 2024) propose a lifelong imitation learning framework for navigation control that includes

054 self-supervised policy and distribution evaluation. However, their method does not explicitly address
 055 the distribution shift problem, making it vulnerable when encountering out-of-distribution states.
 056

057 In this paper, we propose a robust offline to adaptive online imitation learning (RAIL) framework to
 058 address the aforementioned problems. During offline training, we utilize not only expert demonstra-
 059 tions but also supplementary demonstrations. We define supplementary demonstrations as trajectories
 060 collected from novices, suboptimal experts, or those automatically generated during agent training
 061 in simulation. All such data are inherently of unknown optimality. A key requirement is that these
 062 demonstrations can be acquired with minimal effort, in contrast to approaches that deliberately
 063 attempt to cover unexplored regions of the state space. These supplementary demonstrations provide
 064 high coverage of the full environment state space to the policy (Fig. 3).

065 To effectively leverage the supplementary demonstrations, we train the agent using a discriminator-
 066 based weighted behavior cloning algorithm inspired by Xu et al. (2022); Li et al. (2023). We first
 067 train a discriminator with the proposed regularization term that distinguishes between expert and
 068 supplementary demonstrations that estimate the optimality of the training samples, and then utilize
 069 it for behavior cloning. In the online phase, we build upon one important insight: from the agent’s
 070 perspective, its online experience can also be regarded as suboptimal demonstrations. Based on this
 071 insight, we adopt the same learning procedure as in the offline phase for online learning. The agent
 072 computes a self-supervised learning signal from its online experience using the discriminator and
 073 updates the policy with behavior cloning. Furthermore, as online learning at every timestep could
 074 negatively impact policy generalization performance (Yoon et al., 2024), we conduct online learning
 075 only when a distribution shift is detected. When the distribution shift happens, we conduct an online
 076 update for both the discriminator and the policy from the online experience.

077 To evaluate RAIL framework, we design an experimental protocol that deploys the robot to the noise-
 078 injected online environment (Ke et al., 2023) to induce distribution shift. We conduct experiments on
 079 MuJoCo environments and demonstrate that our proposed method outperforms baseline algorithms
 in both the offline and online phases. The contributions of our paper are summarized as follows:

- 080 1. We propose a robust offline to adaptive online imitation learning framework that comprehen-
 081 sively addresses the distribution shift in a lifelong, multi-phase scheme.
- 082 2. We propose a regularization term for the discriminator that enables the discriminator to
 083 estimate the optimality of input data samples more accurately.
- 084 3. We present an adaptive online learning method in which the agent computes self-supervision
 085 signals from online experiences using the discriminator, and performs online learning only
 086 when a distribution shift is detected for stable adaptation.

088 2 RELATED WORKS

091 2.1 IMITATION LEARNING AGAINST DISTRIBUTION SHIFT

092 There are several studies that handles the distribution shift problem by making the policy robust
 093 to the distribution shift. Mehta et al. (Mehta et al., 2025) proposed to incorporate environment
 094 dynamics into the training process to improve policy robustness against distribution shift, which
 095 focus on the policy optimization procedure. The other way is to expand the dataset to encourage
 096 the policy to visit a broader range of states during training. Specifically, expert demonstrations
 097 can be collected by perturbing human operators and recording their recovery behavior, thereby
 098 providing demonstrations that are inherently more robust to distribution shift (Laskey et al., 2017a;
 099 Umut Ciftci et al., 2024). Another approach involves training a world model from the demonstrations
 100 and generating model-based virtual rollouts to augment the offline dataset (Chang et al., 2021; Ke
 101 et al., 2023). Nevertheless, these methods suffer from inherent drawbacks, such as the high cost of
 102 acquiring expert demonstrations or vulnerability to modeling errors in the learned world models.

103 **Moreover, it is nearly impossible to include or model the infinitely many variables that may arise**
 104 **during the online phase within the offline dataset.** In other words, distribution shift is inevitable
 105 during online inference, highlighting the necessity of online learning to address it. One of the most
 106 widely adopted approaches is RL (Schulman et al., 2015), which leverages various exploration
 107 strategies (Yoon et al., 2020) to obtain self-supervision learning signals for online learning. However,
 given that exploration is prohibited during inference due to operational stability or safety constraints,

108 adapting the policy through RL is undesirable. Furthermore, RL is fundamentally ill-suited for
 109 instant adaptation because the reward signals are often delayed, resulting in slow and unstable policy
 110 updates (Zhu et al., 2022). Upon this problem, several RL-based online imitation learning (Ho &
 111 Ermon, 2016; Yue et al., 2024) are also not desirable for the adaptation, although they can compute
 112 a self-supervision signal with a discriminator. Another line of research explores lifelong behavior
 113 cloning. Gong et al. (Gong et al., 2024) proposed computing a self-supervised behavior cloning
 114 signal for online experiences by evaluating both the policy and the distribution. However, their
 115 approach explicitly compares the online experience with the training dataset to measure novelty,
 116 which struggles to distinguish between experiences arising from distribution shift. As a result, it often
 117 fails to correctly adapt, primarily due to the difficulty in accurately computing the self-supervised
 118 learning signal.

119 In this paper, we propose a lifelong scheme robust offline to adaptive online imitation learning frame-
 120 work that addresses distribution shift by sequential mechanisms: first, by leveraging supplementary
 121 demonstrations with a proposed discriminator function during the offline phase to improve robustness
 122 to distribution shift; and second, by computing a self-supervised learning signal with the discriminator
 123 and update the policy in a stable manner to solve distribution shift during the online inference phase.
 124 **In general, the target robot in which robotic intelligence performs inference are fixed. Thus, from**
 125 **the perspective of robot intelligence, the most practically encountered form of distribution shift is**
 126 **covariate shift. Accordingly, this work focuses on addressing this covariate shift.**

127 2.2 LEVERAGING SUPPLEMENTARY DEMONSTRATIONS IN IMITATION LEARNING

128 There are previous studies that utilize supplementary demonstrations for offline imitation learning
 129 based on the problem definition that obtaining expert demonstrations is costly (Wang et al., 2023;
 130 Xu et al., 2022; Li et al., 2023). These studies train a discriminator that can distinguish between
 131 expert demonstrations and supplementary demonstrations, and perform weighted behavior cloning
 132 based on it (Xu et al., 2022). In particular, Li et al. (Li et al., 2023) applied importance weights when
 133 training the discriminator to accurately assess the importance of each demonstration. It theoretically
 134 proves that if the offline dataset covers the stationary state-action distribution of the expert policy by
 135 leveraging population-level supplementary demonstrations, policy performance can be guaranteed.
 136 Furthermore, in the context of online learning, Wang et al. (Wang et al., 2021a) and Liu et al.
 137 (Liu et al., 2025) address the issue that expert demonstrations may contain sub-optimal behaviors.
 138 Wang et al. (Wang et al., 2021a) introduces a method that addresses this by adjusting weights
 139 accordingly, while Liu et al. (Liu et al., 2025) proposed a similar approach. The core idea behind
 140 such methodologies lies in accurately estimating the level of expertise for each training sample by
 141 effectively learning the discriminator. However, a common issue is that the discriminator often
 142 fails to learn properly in the early stages of training or when the dataset is insufficient, leading to
 143 unstable learning. To address this problem, we introduce a regularization term designed to stabilize
 144 the discriminator’s learning and improve overall performance. A detailed analysis of this approach is
 145 provided in Sec. 3.

146 3 WEIGHTED BEHAVIOR CLONING WITH DISCRIMINATOR

147 Behavior Cloning (BC) is one of the representative algorithms in imitation learning, known to enable
 148 more stable and immediate training compared to adversarial imitation learning. The generalized
 149 objective function of BC can be defined as eq. (1):

$$153 \min_{\pi} \mathbb{E}_{(s,a) \sim D_O} [-\omega(s,a) \log \pi(a|s)] \quad (1)$$

154 where D_O indicates the overall training dataset. This maximizes the log likelihood between the
 155 policy’s chosen action and the ground truth at a given state, where the weight $\omega(s,a)$ is calculated
 156 based on the optimality of the current state-action pair. For expert demonstration pairs, $\omega(s,a)$ is set
 157 to 1, while for the worst demonstrations, it is set to 0. For intermediate optimality, $\omega(s,a)$ takes a
 158 continuous value between 0 and 1. Thus, accurately measuring the optimality of demonstrations to
 159 set $\omega(s,a)$ is critical when training policies with BC. This optimality can be assigned either manually
 160 by humans or through discriminators. (Xu et al., 2022; Li et al., 2023) utilizes the discriminator to
 161 estimate the optimality of the offline dataset, and we build our framework upon these methods.

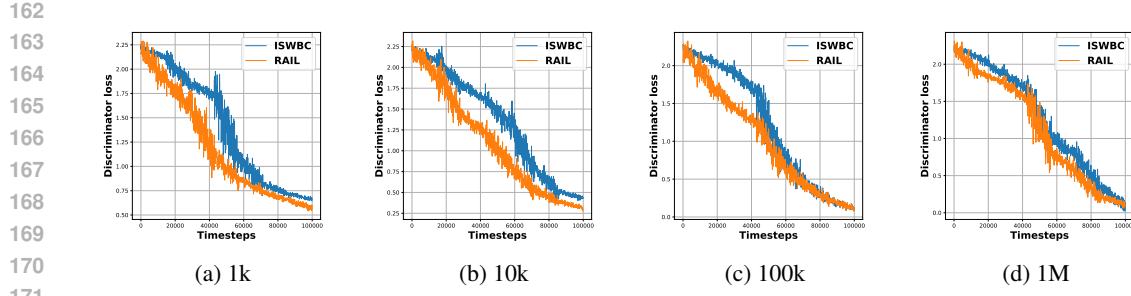


Figure 1: Discriminator evaluation loss for different sizes of expert demonstrations. The number indicated in each subcaption corresponds to the number of expert demonstrations utilized in our experiments while the number of supplementary demonstration is fixed to 1M. The x-axis of each figure denotes the training timesteps of the discriminator, while the y-axis represents the evaluation loss. Across all figures, especially in (a) - (c) that imbalance exists, it is evident that the proposed discriminator exhibits more stable and faster convergence, and also better discriminating performance compared to the baseline.

Discriminator is a strong tool to discriminate between the expert and supplementary demonstrations; however, there are several challenges in practice. When expert and supplementary demonstrations are severely imbalanced, owing to the relative ease of collecting supplementary data, the learned discriminator is prone to developing a biased decision boundary. (Arjovsky & Bottou, 2017; Mao et al., 2017). Moreover, with finite expert datasets, estimating the underlying density ratio suffers from high variance, making importance-weighted policy learning unreliable (Sugiyama et al., 2007; Thomas & Brunskill, 2016). In particular, (Li et al., 2023) assumed the population amount of the offline dataset that covers the stationary state-action distribution of the expert, which is hard to satisfy for most of the real tasks (Yue et al., 2024). This phenomenon is particularly pronounced during the early stages of discriminator training (Kiryo et al., 2017; du Plessis et al., 2016). We conduct empirical analysis about this problem, and the results are explained in Fig. 1. The core of our study lies in identifying the limitations of discriminators commonly used in online imitation learning or offline imitation learning that leverages supplementary demonstrations (Ho & Ermon, 2016; Yue et al., 2024; Li et al., 2023), and to address these limitations, we propose an improved discriminator objective by introducing a novel regularization term.

4 PROPOSED METHODS

4.1 METHOD SETTING AND OVERVIEW

We build our method on the fully observed Markov Decision Process (MDP) setting. MDP is defined by the tuple $M = (\mathcal{S}, \mathcal{A}, P, R, \mu, \gamma)$, where \mathcal{S} is the state space, \mathcal{A} is the action space, $T : \mathcal{S} \times \mathcal{A} \rightarrow \Delta(\mathcal{S})$ is the state transition dynamics, R is the reward function, μ is the initial state distribution, and γ is the discount factor. All policies in this paper are designed to be stochastic, based on Gaussian parameterizations as $\pi_\theta(a | s) = \prod_{i=1}^d \mathcal{N}(a_i; \mu_{\theta,i}(s), \sigma_{\theta,i}^2(s))$ which is parameterized by θ . To train the policy, we have two types of offline datasets. The first is expert demonstrations $D_E = \{(s_E^{i,j}, a_E^{i,j})\}_{i=1}^{N_E}$, collected from an expert policy, which enable the agent to imitate expert behavior, where N_E indicates the number of the trajectories in expert demonstration and i indicates the index of the trajectory and j indicates the index of the sample. The second is supplementary demonstrations $D_S = \{(s_S^{i,j}, a_S^{i,j})\}_{i=1}^{N_S}$, collected from a policy with unknown optimality, used to expand the state-action space coverage during offline training so that improve robustness to distribution shift. N_S indicates the number of the trajectories in the supplementary demonstration. Using these demonstrations, we build our robust offline to adaptive online imitation learning (RAIL) framework that consists of two phases: the offline training and the online inference phase.

216 4.2 OFFLINE TRAINING PHASE: ROBUST IMITATION LEARNING
217

218 The main focus of the offline training phase is to effectively and stably train the policy using both
219 expert demonstrations and optimality-unknown supplementary demonstrations. To this end, we draw
220 inspiration from prior works (Xu et al., 2022; Li et al., 2023) and train a discriminator that can clearly
221 distinguish between D_E and D_S , i.e., determine the optimality of a given state-action pair provided
222 to the training policy. Specifically, we formulate our discriminator loss function based on vanilla
223 discriminator loss function as eq. (2) (Li et al., 2023).

$$225 L_{\text{disc}}^{\text{off}} = \mathbb{E}_{(s,a) \sim D_E} [-\log d(s,a)] + \mathbb{E}_{(s,a) \sim D_S} [-\frac{\widehat{d}_h^S(s,a)}{\widehat{d}_h^E(s,a)} \log(1 - d(s,a))] \quad (2)$$

228 Here, $\widehat{d}_h^E(s,a)$ denotes the empirical state-action distribution of expert demonstrations, and $\widehat{d}_h^S(s,a)$
229 denotes that of supplementary demonstrations. It has been theoretically established that training
230 the discriminator using the objective in eq. (2) enables binary classification between expert and
231 supplementary demonstrations (Li et al., 2023; Ho & Ermon, 2016). Based on this, the discriminator
232 output $d(s,a)$ and its optimal value $d^*(s,a)$ is computed as $d(s,a) = \frac{\widehat{d}_h^E(s,a)}{\widehat{d}_h^E(s,a) + \widehat{d}_h^S(s,a)}$, $d^*(s,a) =$
233 $\frac{\widehat{d}_h^E(s,a)}{\widehat{d}_h^E(s,a) + \widehat{d}_h^S(s,a)}$, where the $d_h^E(s,a)$ and $d_h^S(s,a)$ are ground-truth of $\widehat{d}_h^E(s,a)$ and $\widehat{d}_h^S(s,a)$, respec-
234 tively, and when trained with population-level demonstrations, $d(s,a)$ can closely approximate the
235 ground-truth value $d^*(s,a)$ (Li et al., 2023). Using this optimized discriminator output, the behavior
236 cloning (BC) weight is derived as $\omega(s,a) = \frac{d^*(s,a)}{1-d^*(s,a)}$ (Li et al., 2023). While these findings are
237 well-organized and have demonstrated strong performance, as analyzed in Sec. 3, the discriminator
238 suffers from unstable training in the early stages, particularly depending on the distribution and
239 quantity of the demonstrations.

240 To handle these limitations, we propose a regularization term that helps the stable and accurate learning
241 of the discriminator. Our method aims to assist or guide the discriminator training by encouraging it
242 to better approximate the empirical state-action distributions $\widehat{d}_h^E(s,a)$ from D_E and $\widehat{d}_h^S(s,a)$ from
243 D_S . Specifically, $\widehat{d}_h^E(s,a)$ corresponds to the empirical probability that a training sample (s,a)
244 originates from D_E , while $\widehat{d}_h^S(s,a)$ denotes the corresponding probability for D_S . These quantities
245 are obtained by directly analyzing the empirical statistics of each dataset, yielding the approximations
246 $\widehat{d}_h^E(s,a) \approx p_E(s,a)$, $\widehat{d}_h^S(s,a) \approx p_S(s,a)$, where $p_E(s,a)$ and $p_S(s,a)$ represent the estimated
247 inclusion probabilities of (s,a) in D_E and D_S , respectively. Based on this formulation, we define the
248 target discriminator output as $d(s,a) = \frac{\widehat{d}_h^E(s,a)}{\widehat{d}_h^E(s,a) + \widehat{d}_h^S(s,a)} \approx \frac{p_E(s,a)}{p_E(s,a) + p_S(s,a)}$, which reflects the relative
249 likelihood that a given state-action pair originates from the expert or not. Therefore, by treating this
250 relative ratio as a form of ground truth for training, the discriminator can be learned more stably
251 compared to relying solely on binary discrimination. To this end, we formulate a regularization term
252 L_{reg} that guides the discriminator to this target structure, as in eq. (3).

$$253 L_{\text{reg}} = \mathbb{E}_{(s,a) \sim D_O} [||d(s,a) - \frac{p_E(s,a)}{p_E(s,a) + p_S(s,a)}||_2^2] \quad (3)$$

254 Next, we focus on computing $p_S(s,a)$ and $p_E(s,a)$. By Bayes’s rule (Murphy, 2022), these can
255 be decomposed as $p_E(s,a) = p_E(a|s)p_E(s)$ and $p_S(s,a) = p_S(a|s)p_S(s)$, respectively. Here,
256 $p_E(a|s)$ is approximated by the action likelihood from an expert policy $\widetilde{\pi}_E(\cdot|s)$ trained solely on D_E
257 and $p_S(a|s)$ is approximated by the action likelihood from a supplementary policy $\widetilde{\pi}_S(\cdot|s)$ trained
258 solely on D_S , i.e., $p_{(\cdot)}(a|s) = \widetilde{\pi}_{(\cdot)}(a|s) = \exp(-\frac{1}{2} \sum_{i=1}^d (\log(2\pi\sigma_i^2(s)) + \frac{(a_i - \mu_i(s))^2}{\sigma_i^2(s)}))$, where
259 $p_{(\cdot)}$ could be p_E or p_S with parameters for each policy. Next, we estimate $p_E(s)$ by clustering
260 the states from D_E , and similarly $p_S(s)$ clustering the states from D_S . We utilize the Gaussian
261 Mixture Model (GMM) approach for clustering. After fitting a GMM for each demonstration
262 dataset, $p_E^{\text{GMM}}(s)$ for D_E and $p_S^{\text{GMM}}(s)$ for D_S , we compute the probabilities that the training
263 state sample is included in the fitted model, i.e., $p_{(\cdot)}^{\text{GMM}}(s) = \sum_{k=1}^K \frac{\pi_k}{(2\pi)^{d/2} |\Sigma_k|^{1/2}} \exp(-\frac{1}{2}(s -$

270

Algorithm 1: RAIL Framework

271

Given: Expert demonstrations D_E , Supplementary demonstrations D_S .

272

Train expert policy $\widehat{\pi}_E$ and supplementary policy $\widehat{\pi}_S$.

273

Estimate gaussian mixture model (GMM) of state s : $p_E^{GMM}(s)$ of D_E and $p_S^{GMM}(s)$ of D_S .

274

Train discriminator ϕ with $L_{\text{final}}^{\text{off}}$.

275

Train π by weighted behavior cloning with eq. (1).

276

while *online inference* **do**

277

if *distribution shift happens* **then**

278

 Collect online experience dataset D_X .

279

 Update ϕ with eq. (4).

280

 Update π with eq. (1).

281

282

283

$\mu_k)^T \Sigma_k^{-1} (s - \mu_k)$ where $p_{(\cdot)}^{GMM}(s)$ could be $p_E^{GMM}(s)$ or $p_S^{GMM}(s)$ with parameters for each fitted model. In summary, our approximated probabilities $p_E(s, a)$ and $p_S(s, a)$ could be estimated as $p_E(s, a) = \widehat{\pi}_E(a|s)p_E^{GMM}(s)$ and $p_S(s, a) = \widehat{\pi}_S(a|s)p_S^{GMM}(s)$.

284

At last, by integrating L_{reg} into the discriminator objective $L_{\text{disc}}^{\text{off}}$, we stabilize the training process and improve the discriminator's ability to distinguish between expert and supplementary samples, leading to more accurate behavior cloning weight estimation. The final form of our proposed discrimination loss function is $L_{\text{final}}^{\text{off}} = L_{\text{disc}}^{\text{off}} + \lambda L_{\text{reg}}$, where λ is the hyperparameter and it decreases as the training proceeds. Since our regularization term employs approximated values, it tends to be particularly beneficial in the initial training phase. At last, based on the output $d^*(s, a)$ from the optimized discriminator, we formulate the behavior cloning weight $\omega(s, a) = \frac{d^*(s, a)}{1 - d^*(s, a)}$, and perform weighted behavior cloning with eq. (1). A detailed theoretical analysis showing that $L_{\text{final}}^{\text{off}}$ enables stable learning is provided in Appendix B.1.

297

298

4.3 ONLINE INFERENCE PHASE: ADAPTATION VIA SELF-SUPERVISED IMITATION LEARNING

299

In the online phase, our core idea is that we solve the distribution shift problem via adaptation to the environment with self-supervised online learning from experience. However, indiscriminately learning from all online experiences is undesirable, as it can degrade the general policy performance (Laroche et al., 2019; Kemker et al., 2018) and also incur significant computational overhead. Therefore, we design a metric to quantify the degree of distribution shift and conduct online learning only when a distribution shift is detected. Based on the definition of distribution shift which comes from unvisited state during offline training, we define the distribution shift detection function as $\kappa(s) = \frac{p_E(s) + p_S(s)}{2}$ where $\kappa(s)$ represents the average likelihood that a given state s belongs to D_E or D_S . Instead of using the Mahalanobis distance, which is suitable for low-dimensional data, our method employs a likelihood-based estimation method that can more effectively measure distribution shift in high-dimensional robotics data (Nayal et al., 2024; Mueller & Hein, 2025). If $\kappa(s)$ falls below a predefined threshold κ_{TH} , we interpret this as an indication of distribution shift, with the severity quantified by $\kappa(s)$.

306

We do not immediately initiate online learning just because a single-step distribution shift is detected. While we expect the learning-based policy to handle distribution shift through its generalization capability, we also set that if distribution shift persists beyond a certain number of timesteps (N_{ds}), the generalization capability of the policy has failed. In such cases, we conduct online learning. We call this as method update time management (UTM). Once a distribution shift is detected, online learning is conducted using the accumulated data D_X collected during the distribution shift occurrence.

313

At last, we describe our policy update strategy for online adaptation. When a distribution shift is detected, we perform online learning using the tuples (s, a) consisting of the encountered states and the actions taken by the policy at those states. From the perspective of the policy, these tuples can be regarded as supplementary demonstrations, therefore, we adopt the same training strategy as in the offline phase. However, we incorporate the degree of distribution shift into the learning process via the $\kappa(s)$ value for adaptive learning. A high $\kappa(s)$ indicates that the corresponding state was likely visited in the offline phase, meaning that it is appropriate to sufficiently affect the discriminator that

324
 325 Table 1: Result of offline training evaluation. The values in the table represent the D4RL scores
 326 obtained by performing inference with the policies trained offline by each method in an online
 327 environment with injected random Gaussian noise. Each score is averaged over 10 runs.

Env	Noise	BC	Stable BC	CCIL	RAIL (Ours)
Hopper	$\sigma = 0$	94.96 (± 0.1)	94.63 (± 0.1)	94.53 (± 0.1)	94.48 (± 0.1)
	$\sigma = 0.05$	61.51 (± 0.3)	82.45 (± 0.2)	85.36 (± 0.2)	85.30 (± 0.3)
	$\sigma = 0.1$	35.97 (± 0.5)	61.45 (± 0.6)	73.07 (± 0.6)	77.06 (± 0.5)
	$\sigma = 0.2$	10.45 (± 1.5)	47.03 (± 1.2)	53.73 (± 1.6)	62.19 (± 1.3)
Halfcheetah	$\sigma = 0$	92.43 (± 0.1)	93.30 (± 0.1)	93.47 (± 0.1)	93.28 (± 0.1)
	$\sigma = 0.05$	48.96 (± 0.2)	74.05 (± 0.3)	84.13 (± 0.2)	89.27 (± 0.3)
	$\sigma = 0.1$	24.91 (± 0.3)	61.02 (± 0.5)	70.05 (± 0.6)	74.07 (± 0.6)
	$\sigma = 0.2$	5.99 (± 1.5)	19.48 (± 1.7)	42.39 (± 1.3)	49.57 (± 1.9)
Walker2d	$\sigma = 0$	109.27 (± 0.1)	108.40 (± 0.1)	108.78 (± 0.1)	108.77 (± 0.1)
	$\sigma = 0.05$	65.77 (± 0.3)	73.49 (± 0.3)	68.06 (± 0.3)	86.19 (± 0.3)
	$\sigma = 0.1$	21.23 (± 0.5)	51.84 (± 0.5)	54.84 (± 0.6)	69.57 (± 0.5)
	$\sigma = 0.2$	1.30 (± 1.1)	24.36 (± 1.7)	22.65 (± 1.1)	48.60 (± 1.3)
Ant	$\sigma = 0$	92.86 (± 0.1)	91.79 (± 0.1)	93.80 (± 0.1)	92.57 (± 0.1)
	$\sigma = 0.05$	39.19 (± 0.2)	52.45 (± 0.3)	59.28 (± 0.2)	68.20 (± 0.2)
	$\sigma = 0.1$	21.81 (± 0.2)	25.56 (± 0.4)	29.78 (± 0.5)	48.68 (± 0.6)
	$\sigma = 0.2$	5.63 (± 1.3)	18.77 (± 1.1)	21.81 (± 1.0)	38.68 (± 1.0)

347 was trained during the offline phase and also allow it to influence the policy (Wang et al., 2021b;a).
 348 Conversely, a low $\kappa(s)$ implies a state far from the offline dataset, and thus the update should be more
 349 conservative. Based on this reasoning, the discriminator objective used during the online phase is
 350 given by eq.(4).

$$L_{\text{disc}}^{\text{on}} = \mathbb{E}_{(s,a) \sim D_E} [-\log d(s,a)] + \mathbb{E}_{(s,a) \sim D_X} [-\kappa(s) \log(1 - d(s,a))] \quad (4)$$

354 After updating the discriminator with $L_{\text{disc}}^{\text{on}}$, we perform weighted behavior cloning using the discriminator
 355 output $d(s, a)$. This approach extends behavior cloning, which was previously limited to offline
 356 imitation learning, to online imitation learning with the assistance of a discriminator. Through this
 357 method, we propose a robust offline to adaptive online imitation learning framework that can com-
 358 prehensively handle the distribution shift problem during both offline training and online inference
 359 phases. The algorithm for the RAIL framework is described in Algorithm 1.

5 EXPERIMENTS

5.1 SETUP

365 Our research is similar to multi-task imitation learning (Zhang et al., 2023) and transfer learning
 366 (Cauderan et al., 2023) in that it continuously learns from new environments or task data. However,
 367 while these studies assume the existence of ground truth expert demonstrations for new tasks, we
 368 assume the absence of ground truth expert demonstrations for the online environment. Therefore,
 369 we conduct offline learning with an offline dataset and design an evaluation protocol by setting an
 370 online environment where a distribution shift occurs. We conduct the evaluation in four environments
 371 from MuJoCo (Hopper, Halfcheetah, Walker2d, and Ant). Expert demonstrations are constructed
 372 from the D4RL dataset (Fu et al., 2021), and supplementary demonstrations are constructed by
 373 mixing all miscellaneous demonstrations (random, medium-replay, medium, medium-expert) from
 374 the D4RL dataset. Moreover, for a unified description about the experiment results, we converted
 375 episode returns to D4RL score instead of using the raw episode returns. During online inference,
 376 random Gaussian noise is added to the state to evoke distribution shift (Laskey et al., 2017b; Mehta
 377 et al., 2025). The intensity of the noise is controlled by adjusting the covariance of the Gaussian
 378 noise $\epsilon \sim \mathcal{N}(0, \sigma^2)$. The noise intensity is set at four levels: $\sigma = 0, 0.05, 0.1, 0.2$. When $\sigma = 0$, it
 379 corresponds to the raw environment without noise, and as the value increases, the intensity of the

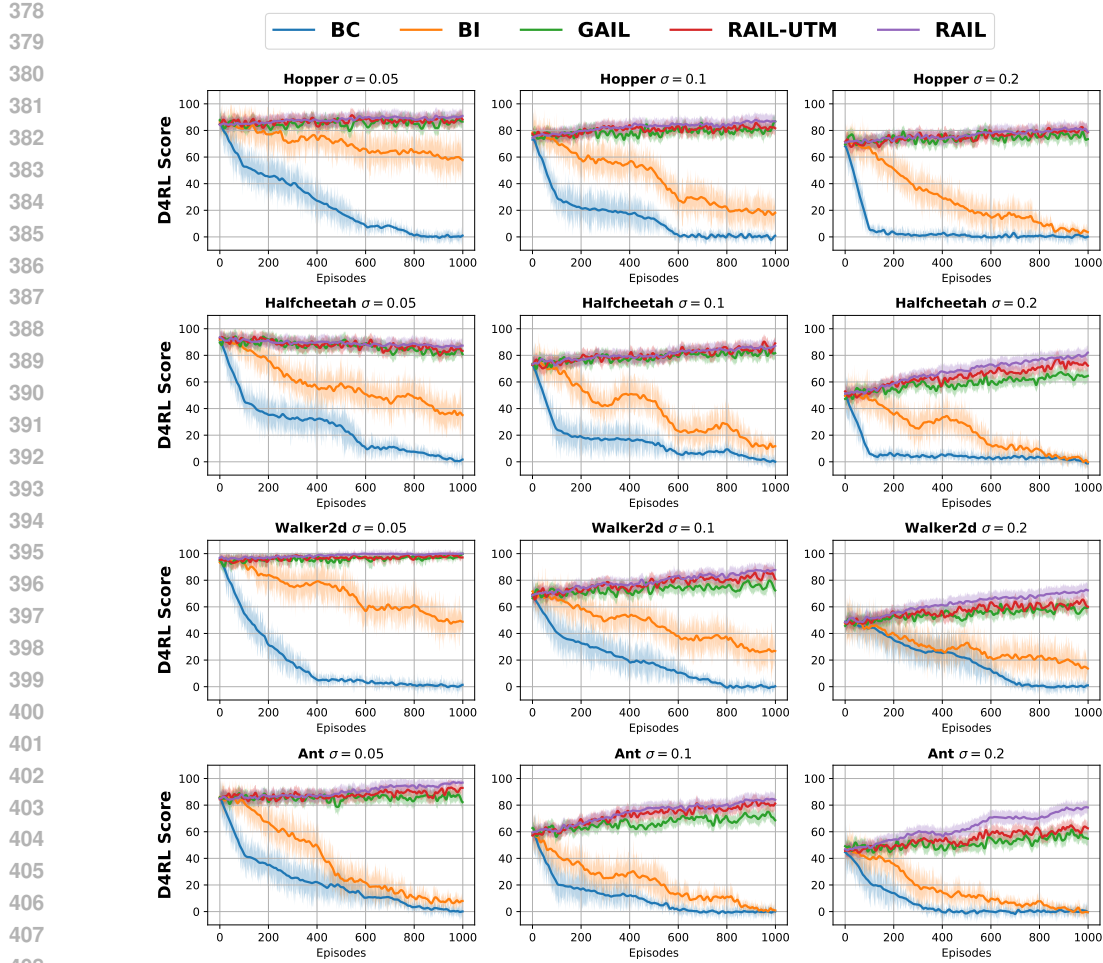


Figure 2: Evaluation for online learning performance.

noise becomes stronger. For online phase, we set κ_{TH} to 0.4 and N_{ds} to 20. We set these values as a hyperparameter and figured them out with a grid-search approach (see Appendix D.2 for details). We conduct policy training using NVIDIA RTX 3090 GPU. Through experiments, we mainly focus on answering the following questions:

- **Question 1 (Offline):** Does leveraging supplementary demonstrations with the proposed discriminator function make the policy robust to the distribution shift?
- **Question 2 (Online):** Does self-supervised online learning make the policy adapt to the current environment and solve the distribution shift?

5.2 RESULTS AND DISCUSSIONS

Answer for Question 1. For the offline phase evaluation to answer question 1, we adopt BC, Stable BC (Mehta et al., 2025), and Model-based BC (Ke et al., 2023) as baselines. Based on the result in Table 1, we can confirm that RAIL consistently achieves the highest single-episode return. When noise σ is 0, the environment is identical to the offline demonstration environment, and thus all methods show similar high performance. However, as σ increases, it becomes evident that data augmentation-based BC algorithms, Model-based BC and RAIL, are more effective than Stable BC, which focuses solely on policy optimization. Based on these results, we observe that while stabilizing policy learning is important, enhancing state coverage proves to be a more effective approach for achieving robustness to distribution shift. Among the data augmentation-based methods, the offline framework of RAIL demonstrates superior performance, verifying that leveraging real supplementary

432 demonstrations with our discriminator is more effective for learning a robust policy than relying on
 433 model-based virtual demonstrations. Based on these results, we can answer Q1 with a "yes."
 434

435 **Answer for Question 2.** Next, for the online phase evaluation to answer question 2, we adopt BC,
 436 Beyond Imitation (BI) (Gong et al., 2024), and GAIL (Ho & Ermon, 2016) as baselines. To ensure
 437 a fair comparison, we initialized each algorithm's policy and, where applicable (i.e., GAIL and
 438 RAIL), the discriminator using the models trained during the offline phase with RAIL. Fig. 2 shows
 439 that RAIL exhibits the most significant performance improvement than other algorithms. **In online**
 440 **phase, BC always treats online experience as expert supervision, leaving no mechanism to mitigate**
 441 **the compounding errors triggered by a incorrect action under distribution shift. Consequently, its**
 442 **performance degrades substantially.** Although BI attempts to estimate self-supervision from online
 443 experience, it fundamentally assumes that the agent alone can obtain a meaningful self-supervised
 444 learning signal during the inference phase, making it vulnerable to distribution shift. In contrast,
 445 methods such as GAIL and RAIL, which compute self-supervised learning signals from online
 446 experience via the discriminator, exhibit performance improvement during online learning. This
 447 implies that they successfully address the distribution shift through adaptation from online learning.
 448 Moreover, better performance of RAIL against GAIL implies that a clear optimality estimation
 449 procedure for online experience is necessary through our regularization term. Besides, we also
 450 evaluated an ablated model, RAIL-UTM, which removes the UTM technique from RAIL and
 451 performs online learning on all online experiences without distribution shift detection. Although
 452 RAIL-UTM outperforms GAIL, it is inferior to RAIL in the overall performance. **Moreover, RAIL not**
 453 **only outperforms RAIL-UTM, but also achieves approximately 54% reduction in training time.** This
 454 result highlights the importance of the UTM technique in achieving efficient and stable adaptation.
 455

456 Additionally, we further analyze GAIL and RAIL in terms of learning stability, which was introduced
 457 in Sec. 2.1. Although both methods compute self-supervised learning signals from online experience
 458 via the discriminator, GAIL updates the policy using TRPO (Schulman et al., 2015), whereas
 459 RAIL updates the policy using weighted BC. Fig. 2 demonstrates that weighted BC enables more
 460 stable policy learning during online adaptation compared to RL. More detailed experimental results
 461 are provided in Appendix C.4. Overall, RAIL consistently outperforms GAIL in terms of final
 462 performance and also guarantees more stable learning and adaptation. These results confirm that
 463 RAIL is more suitable than GAIL for achieving stable performance improvement during inference-
 464 time adaptation. Thus, we can answer Q2 with a "yes."

465 We further investigated the impact of supplementary demonstration coverage, with results presented
 466 in Appendix C.2. The results show that broader coverage—even from low-optimality data such
 467 as random policies—consistently outperforms using only suboptimal demonstrations with near-
 468 expert quality. This confirms that coverage, alongside optimality, is critical for policy learning and
 469 substantiates the soundness of our approach.

470 **Summary.** Through these extensive evaluations, we verify the effectiveness of our RAIL framework,
 471 a unified offline to online lifelong imitation learning framework. The results ensure that with training
 472 and deploying the robot with the RAIL framework, the robot policy becomes robust to distribution
 473 shift during the offline phase (to prevent distribution shift) and adapts to the online environment
 474 during the online phase (to solve distribution shift).

475 6 CONCLUSION

476 We propose RAIL framework that solves the distribution shift problem of imitation learning-based
 477 policy for both offline and online phase in a lifelong scheme. The key idea of our approach is to
 478 leverage supplementary demonstrations to expand the coverage of visited states during offline training.
 479 To efficiently leverage the supplementary demonstrations, we train a discriminator with regularization
 480 that estimates the optimality of training samples based on approximated probability density functions
 481 derived from expert and supplementary demonstrations. This discriminator is then used to compute
 482 BC weights, which are applied to both offline and online learning phases, enabling seamless lifelong
 483 policy training. Furthermore, by triggering online learning only when a clear distribution shift is
 484 detected, our method ensures more stable policy updates. Extensive experiments in the Mujoco
 485 environment validate the effectiveness of the RAIL framework.

486 REPRODUCIBILITY STATEMENT
487

488 We made extensive efforts to enhance the reproducibility of this work. The overall algorithm is
489 summarized in Algorithm 1, and the proofs required for the method are provided in Appendix B.2. In
490 addition, details regarding the model architecture and hyperparameters are described in Appendix D.1.
491 Furthermore, by explicitly incorporating various details throughout the main text, we strived to
492 maximize the reproducibility of our study.

494 REFERENCES
495

496 Trevor Ablett, Bryan Chan, and Jonathan Kelly. Learning from guided play: Improving exploration
497 for adversarial imitation learning with simple auxiliary tasks. *IEEE Robotics and Automation
498 Letters*, 8(3):1263–1270, 2023. doi: 10.1109/LRA.2023.3236882.

499 Martin Arjovsky and Léon Bottou. Towards principled methods for training generative adversarial
500 networks, 2017. URL <https://arxiv.org/abs/1701.04862>.

501 Alvaro Cauderan, Gauthier Boeshertz, Florian Schwab, and Calvin Zhang. Zero-shot transfer in
502 imitation learning, 2023. URL <https://arxiv.org/abs/2310.06710>.

504 Jonathan Chang, Masatoshi Uehara, Dhruv Sreenivas, Rahul Kidambi, and Wen Sun. Mitigating
505 covariate shift in imitation learning via offline data with partial coverage. *Advances in Neural
506 Information Processing Systems*, 34:965–979, 2021.

507 Jinwoo Choi and Seung-Woo Seo. Dynamic contrastive skill learning with state-transition based skill
508 clustering and dynamic length adjustment. In *The Thirteenth International Conference on Learning
509 Representations*, 2025. URL <https://openreview.net/forum?id=8egnwady4b>.

511 Marthinus C. du Plessis, Gang Niu, and Masashi Sugiyama. Class-prior estimation for learning
512 from positive and unlabeled data. *Machine Learning*, 106(4):463–492, November 2016.
513 ISSN 1573-0565. doi: 10.1007/s10994-016-5604-6. URL <http://dx.doi.org/10.1007/s10994-016-5604-6>.

515 Justin Fu, Aviral Kumar, Ofir Nachum, George Tucker, and Sergey Levine. D4rl: Datasets for deep
516 data-driven reinforcement learning, 2021. URL <https://arxiv.org/abs/2004.07219>.

518 Zipeng Fu, Tony Z. Zhao, and Chelsea Finn. Mobile aloha: Learning bimanual mobile manipulation
519 with low-cost whole-body teleoperation. In *Conference on Robot Learning (CoRL)*, 2024.

520 Cheng Gong, Chao Lu, Zirui Li, Zhe Liu, Jianwei Gong, and Xuemei Chen. Beyond imitation:
521 A life-long policy learning framework for path tracking control of autonomous driving. *IEEE
522 Transactions on Vehicular Technology*, 73(7):9786–9799, 2024. doi: 10.1109/TVT.2024.3382309.

524 Jonathan Ho and Stefano Ermon. Generative adversarial imitation learning, 2016. URL <https://arxiv.org/abs/1606.03476>.

526 Liyiming Ke, Yunchu Zhang, Abhay Deshpande, Siddhartha Srinivasa, and Abhishek Gupta.
527 Ceil: Continuity-based data augmentation for corrective imitation learning. *arXiv preprint
528 arXiv:2310.12972*, 2023.

530 Ronald Kemker, Marc McClure, Angelina Abitino, Tyler Hayes, and Christopher Kanan. Measuring
531 catastrophic forgetting in neural networks. In *Proceedings of the AAAI conference on artificial
532 intelligence*, volume 32, 2018.

533 Ryuichi Kiryo, Gang Niu, Marthinus C. du Plessis, and Masashi Sugiyama. Positive-unlabeled
534 learning with non-negative risk estimator, 2017. URL <https://arxiv.org/abs/1703.00593>.

536 Romain Laroche, Paul Trichelair, and Rémi Tachet des Combes. Safe policy improvement with
537 baseline bootstrapping, 2019. URL <https://arxiv.org/abs/1712.06924>.

539 Michael Laskey, Jonathan Lee, Roy Fox, Anca Dragan, and Ken Goldberg. Dart: Noise injection for
robust imitation learning. In *Conference on robot learning*, pp. 143–156. PMLR, 2017a.

540 Michael Laskey, Jonathan Lee, Roy Fox, Anca Dragan, and Ken Goldberg. Dart: Noise injection for
 541 robust imitation learning, 2017b. URL <https://arxiv.org/abs/1703.09327>.

542

543 Ziniu Li, Tian Xu, Zeyu Qin, Yang Yu, and Zhi-Quan Luo. Imitation learning from imperfection:
 544 Theoretical justifications and algorithms. In *Thirty-seventh Conference on Neural Information
 545 Processing Systems*, 2023. URL <https://openreview.net/forum?id=v004AzsB49>.

546

547 Qiang Liu, Huiqiao Fu, Kaiqiang Tang, Chunlin Chen, and Daoyi Dong. Pn-gail: Leveraging non-
 548 optimal information from imperfect demonstrations. In *The Thirteenth International Conference
 549 on Learning Representations*, 2025.

550

551 Xudong Mao, Qing Li, Haoran Xie, Raymond Y. K. Lau, Zhen Wang, and Stephen Paul Smolley.
 552 Least squares generative adversarial networks, 2017. URL <https://arxiv.org/abs/1611.04076>.

553

554 Shaunak A Mehta, Yusuf Umut Ciftci, Balamurugan Ramachandran, Somil Bansal, and Dylan P
 555 Losey. Stable-bc: Controlling covariate shift with stable behavior cloning. *IEEE Robotics and
 556 Automation Letters*, 2025.

557

558 Maximilian Mueller and Matthias Hein. Mahalanobis++: Improving ood detection via feature
 559 normalization, 2025. URL <https://arxiv.org/abs/2505.18032>.

560

561 Kevin P Murphy. *Probabilistic machine learning: an introduction*. MIT press, 2022.

562

563 Nazir Nayal, Youssef Shoeb, and Fatma Güney. A likelihood ratio-based approach to segmenting
 564 unknown objects, 2024. URL <https://arxiv.org/abs/2409.06424>.

565

566 Kishan Panaganti, Zaiyan Xu, Dileep Kalathil, and Mohammad Ghavamzadeh. Distributionally
 567 robust behavioral cloning for robust imitation learning. In *2023 62nd IEEE Conference on Decision
 568 and Control (CDC)*, pp. 1342–1347, 2023. doi: 10.1109/CDC49753.2023.10383976.

569

570 John Schulman, Sergey Levine, Pieter Abbeel, Michael Jordan, and Philipp Moritz. Trust region
 571 policy optimization. In *International conference on machine learning*, pp. 1889–1897. PMLR,
 572 2015.

573

574 Masashi Sugiyama, Matthias Krauledat, and Klaus-Robert Müller. Covariate shift adaptation by
 575 importance weighted cross validation. *Journal of Machine Learning Research*, 8(5), 2007.

576

577 Philip Thomas and Emma Brunskill. Data-efficient off-policy policy evaluation for reinforcement
 578 learning. In Maria Florina Balcan and Kilian Q. Weinberger (eds.), *Proceedings of The 33rd
 579 International Conference on Machine Learning*, volume 48 of *Proceedings of Machine Learning
 580 Research*, pp. 2139–2148, New York, New York, USA, 20–22 Jun 2016. PMLR. URL <https://proceedings.mlr.press/v48/thomas16.html>.

581

582 Yusuf Umut Ciftci, Zeyuan Feng, and Somil Bansal. Safe-gil: Safety guided imitation learning. *arXiv
 583 e-prints*, pp. arXiv–2404, 2024.

584

585 Qiang Wang, Robert McCarthy, David Cordova Bulens, Kevin McGuinness, Noel E. O’Connor,
 586 Francisco Roldan Sanchez, Nico Görtler, Felix Widmaier, and Stephen J. Redmond. Improving
 587 behavioural cloning with positive unlabeled learning. In *7th Annual Conference on Robot Learning*,
 588 2023. URL <https://openreview.net/forum?id=0mRSANSzEK>.

589

590 Yunke Wang, Chang Xu, Bo Du, and Honglak Lee. Learning to weight imperfect demonstrations. In
 591 *International Conference on Machine Learning*, pp. 10961–10970. PMLR, 2021a.

592

593 Yunke Wang, Chang Xu, Bo Du, and Honglak Lee. Learning to weight imperfect demonstrations. In
 594 Marina Meila and Tong Zhang (eds.), *Proceedings of the 38th International Conference on Machine
 595 Learning*, volume 139 of *Proceedings of Machine Learning Research*, pp. 10961–10970. PMLR,
 596 18–24 Jul 2021b. URL <https://proceedings.mlr.press/v139/wang21aa.html>.

597

598 Haoran Xu, Xianyuan Zhan, Honglei Yin, and Huijing Qin. Discriminator-weighted offline imitation
 599 learning from suboptimal demonstrations, 2022. URL <https://arxiv.org/abs/2207.10050>.

594 Hyung-Suk Yoon, Sang-Hyun Lee, and Seung-Woo Seo. Exploration strategy based on validity of
 595 actions in deep reinforcement learning. In *2020 IEEE/RSJ International Conference on Intelligent
 596 Robots and Systems (IROS)*, pp. 6134–6139, 2020. doi: 10.1109/IROS45743.2020.9341014.

598 Hyung-Suk Yoon, Ji-Hoon Hwang, Chan Kim, E In Son, Se-Wook Yoo, and Seung-Woo Seo.
 599 Adaptive robot traversability estimation based on self-supervised online continual learning in
 600 unstructured environments. *IEEE Robotics and Automation Letters*, 9(6):4902–4909, 2024. doi:
 601 10.1109/LRA.2024.3386451.

602 Tianhe Yu, Garrett Thomas, Lantao Yu, Stefano Ermon, James Zou, Sergey Levine, Chelsea Finn,
 603 and Tengyu Ma. Mopo: Model-based offline policy optimization, 2020. URL <https://arxiv.org/abs/2005.13239>.

604 Sheng Yue, Xingyuan Hua, Ju Ren, Sen Lin, Junshan Zhang, and Yaoxue Zhang. Ollie: Imitation
 605 learning from offline pretraining to online finetuning, 2024. URL <https://arxiv.org/abs/2405.17477>.

606 Thomas T. Zhang, Katie Kang, Bruce D. Lee, Claire Tomlin, Sergey Levine, Stephen Tu, and
 607 Nikolai Matni. Multi-task imitation learning for linear dynamical systems, 2023. URL <https://arxiv.org/abs/2212.00186>.

608 Zhuangdi Zhu, Kaixiang Lin, Bo Dai, and Jiayu Zhou. Self-adaptive imitation learning: Learning
 609 tasks with delayed rewards from sub-optimal demonstrations. *Proceedings of the AAAI Conference
 610 on Artificial Intelligence*, 36(8):9269–9277, Jun. 2022. doi: 10.1609/aaai.v36i8.20914. URL
 611 <https://ojs.aaai.org/index.php/AAAI/article/view/20914>.

612 A MOTIVATION OF LEVERAGING SUPPLEMENTARY DEMONSTRATIONS

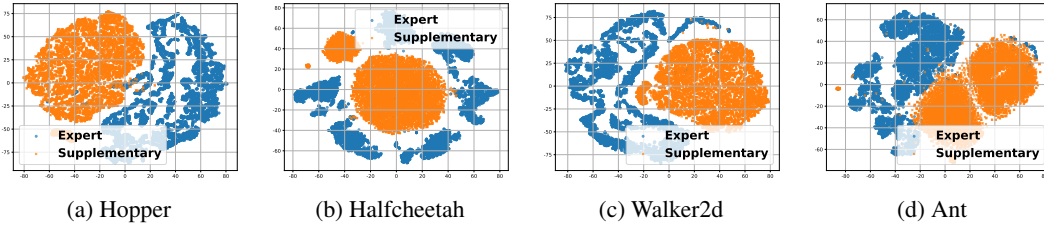


Figure 3: t-SNE plot of the state of the expert and supplementary demonstrations of the Mujoco environment. We observe a clear discrepancy between the state distributions of expert demonstrations and supplementary demonstrations.

As shown in Fig. 3, the supplementary demonstrations and expert demonstrations cover distinct regions of the dataset. This indicates that many state–action pairs that are absent in the expert demonstrations are abundantly present in the supplementary demonstrations. Leveraging this observation, we devised a method to proactively mitigate distribution shift.

646 B THEORETICAL ANALYSIS

647 B.1 POSTERIOR-REGULARIZED DISCRIMINATOR UNDER EXPERT-SUPPLEMENTARY 648 IMBALANCE

In this subsection, we provide a theoretical analysis showing that the proposed regularized discriminator effectively mitigates the biased decision boundary caused by the imbalance between expert and supplementary demonstrations, thereby enabling stable convergence toward the optimal value d^* .

648 **Bayes-optimal discriminator and unbiased decision boundary.** Let $p_E(s, a)$ and $p_S(s, a)$ denote
 649 the true state-action densities of the expert and supplementary demonstrations, respectively. We
 650 consider the binary classification problem of predicting whether a given (s, a) originates from p_E or
 651 p_S . Assuming equal class priors, the Bayes-optimal posterior is

$$653 \quad \eta^*(s, a) := \mathbb{P}(y = 1 \mid s, a) = \frac{p_E(s, a)}{p_E(s, a) + p_S(s, a)}. \quad (5)$$

655 The corresponding decision boundary is

$$656 \quad \mathcal{B}^* := \{(s, a) \mid \eta^*(s, a) = \frac{1}{2}\} = \{(s, a) \mid p_E(s, a) = p_S(s, a)\}. \quad (6)$$

658 Any discriminator $d(s, a) \in (0, 1)$ that aims to correctly separate the expert and supplementary
 659 regions should satisfy $d(s, a) \approx \eta^*(s, a)$, in which case its induced boundary $\mathcal{B}_d := \{(s, a) \mid
 660 d(s, a) = \frac{1}{2}\}$ approximates \mathcal{B}^* .

661 **Effect of class imbalance on the standard adversarial loss.** In practice, the discriminator is
 662 trained on empirical distributions q_E and q_S induced by the finite datasets D_E and D_S . When
 663 $|D_S| \gg |D_E|$, their empirical class priors are highly imbalanced, which we express as

$$664 \quad q_E(s, a) = \alpha_E p_E(s, a), \quad q_S(s, a) = \alpha_S p_S(s, a), \quad \alpha_S \gg \alpha_E > 0. \quad (7)$$

666 The standard discriminator objective is

$$667 \quad L_{\text{std}}(d) = \mathbb{E}_{(s, a) \sim q_E}[-\log d(s, a)] + \mathbb{E}_{(s, a) \sim q_S}[-\log(1 - d(s, a))]. \quad (8)$$

668 Pointwise minimization yields the unique optimal discriminator

$$670 \quad d_{\text{std}}^*(s, a) = \frac{\alpha_E p_E(s, a)}{\alpha_E p_E(s, a) + \alpha_S p_S(s, a)} = \frac{p_E(s, a)}{p_E(s, a) + \beta p_S(s, a)}, \quad \beta := \alpha_S / \alpha_E \gg 1. \quad (9)$$

672 Its decision boundary is

$$673 \quad \mathcal{B}_{\text{std}} = \{(s, a) \mid p_E(s, a) = \beta p_S(s, a)\}, \quad (10)$$

674 which is shifted away from \mathcal{B}^* by the imbalance factor β . Thus, the standard adversarial training
 675 objective induces a biased decision boundary whenever $\alpha_S \neq \alpha_E$.

677 **Posterior-regularized discriminator.** To correct this imbalance-induced distortion, we introduce
 678 the regularized objective

$$679 \quad L_{\text{reg}}(d) = \mathbb{E}_{(s, a) \sim q_E}[-\log d(s, a)] + \mathbb{E}_{(s, a) \sim q_S}[-\log(1 - d(s, a))] \\ 680 \quad + \lambda \mathbb{E}_{(s, a) \sim q_{\text{mix}}}[(d(s, a) - \eta^*(s, a))^2], \quad (11)$$

682 where q_{mix} is any mixing distribution over $D_E \cup D_S$ and we note $\frac{p_E(s, a)}{p_E(s, a) + p_S(s, a)}$ as $\eta^*(s, a)$ for
 683 readability. The added term explicitly penalizes the squared deviation between the discriminator output
 684 and the Bayes-optimal posterior.

686 For a fixed (s, a) , the local objective is

$$687 \quad \ell_{\text{reg}}(d; s, a) = -\alpha_E p_E(s, a) \log d - \alpha_S p_S(s, a) \log(1 - d) + \lambda \gamma(s, a)(d - \eta^*(s, a))^2, \quad (12)$$

688 where $\gamma(s, a) := q_{\text{mix}}(s, a)$. The optimal discriminator $d^*(s, a)$ satisfies the stationarity condition

$$690 \quad -\frac{\alpha_E p_E(s, a)}{d^*} + \frac{\alpha_S p_S(s, a)}{1 - d^*} + 2\lambda \gamma(s, a)(d^* - \eta^*(s, a)) = 0. \quad (13)$$

692 Two limiting regimes follow immediately:

694 • **Limit $\lambda \rightarrow 0$.** Equation equation 13 reduces to the standard case, giving

$$696 \quad d^*(s, a) = d_{\text{std}}^*(s, a) = \frac{p_E(s, a)}{p_E(s, a) + \beta p_S(s, a)}.$$

698 • **Limit $\lambda \rightarrow \infty$.** The quadratic penalty dominates, forcing

$$700 \quad d^*(s, a) \rightarrow \eta^*(s, a) = \frac{p_E(s, a)}{p_E(s, a) + p_S(s, a)}.$$

701 Hence, the induced boundary \mathcal{B}_{reg} converges to the unbiased boundary \mathcal{B}^* .

702 For finite $\lambda > 0$, the minimizer of equation 13 lies between the imbalance-distorted optimum d_{imb}^*
 703 and the Bayes posterior η^* . Locally approximating the cross-entropy term by a quadratic around
 704 $d_{\text{imb}}^*(s, a)$ gives

$$705 \quad d^*(s, a) \approx \frac{w_{\text{CE}}(s, a) d_{\text{imb}}^*(s, a) + w_{\text{R}}(s, a) \eta^*(s, a)}{w_{\text{CE}}(s, a) + w_{\text{R}}(s, a)}, \quad (14)$$

707 for positive weights w_{CE} and w_{R} depending on $\alpha_E, \alpha_S, \lambda, \gamma(s, a)$. Thus, posterior regularization
 708 systematically pulls d^* toward the unbiased Bayes posterior, reducing the boundary distortion.
 709

710 **Practical implementation via density approximation (Main proposed method).** In practice, the
 711 true densities p_E and p_S are unknown, so the Bayes posterior η^* cannot be computed exactly. Instead,
 712 we estimate the densities using a Gaussian Mixture Model (GMM) combined with a neural network
 713 encoder, obtaining consistent approximations \hat{p}_E, \hat{p}_S and the corresponding posterior

$$715 \quad \hat{\eta}(s, a) := \frac{\hat{p}_E(s, a)}{\hat{p}_E(s, a) + \hat{p}_S(s, a)}.$$

717 Replacing η^* with $\hat{\eta}$ in equation 11 yields the empirical regularized objective. Under standard
 718 assumptions (e.g., pointwise consistency of density estimators), $\hat{\eta}(s, a) \rightarrow \eta^*(s, a)$, implying

$$719 \quad d^*(s, a) \xrightarrow{\lambda \rightarrow \infty} \hat{\eta}(s, a) \xrightarrow{\text{consistency}} \eta^*(s, a).$$

721 Therefore, the proposed regularizer recovers the Bayes-optimal discriminator in the limit while
 722 providing a robust finite-sample correction that mitigates the biased decision boundary induced by
 723 expert-supplementary demonstrations imbalance.
 724

725 B.2 IS THE APPROXIMATE PDF REALLY THE JOINT PDF?

727 Without loss of generality, we focus our exposition on the expert demonstrations. Let $D_E =$
 728 $\{(s_i, a_i)\}_{i=1}^N$ denote the dataset collected from expert behavior, where each tuple (s_i, a_i) represents
 729 a state-action pair. Our objective is to estimate the likelihood that a training dataset (s, a) originates
 730 from the expert-induced distribution. To facilitate this, we consider an approximation of the joint
 731 probability distribution as follows:

$$732 \quad p_E(s, a) = p_E(a|s) \cdot p_E(s) \approx \pi_E(a|s) \cdot p_E(s) \quad (15)$$

734 where:

- 736 • $\pi_E(a|s)$ is the expert policy, trained from expert demonstrations D_E , representing the
 737 likelihood of action a of the expert for a given state s ,
- 738 • $p_E(s)$ is the marginal state distribution estimated from D_E , e.g., via Gaussian Mixture
 739 Model in this paper.

741 VALIDITY AS A JOINT PROBABILITY DENSITY FUNCTION

743 We verify that our approximated probability density function $p_E(s, a) = \pi_E(a|s) \cdot p_E(s)$ satisfies
 744 the requirements of a valid joint probability density function.

746 **1. Non-negativity** By the definitions of conditional and marginal probability densities,

$$747 \quad \pi_E(a|s) \geq 0, \quad p_E(s) \geq 0 \quad \Rightarrow \quad p_E(s, a) \geq 0 \quad \forall(s, a)$$

749 **2. Normalization** We must show that the integral over the full space equals 1:

$$751 \quad \int_S \int_A p_E(s, a) da ds = \int_S \left[p_E(s) \int_A \pi_E(a|s) da \right] ds \quad (16)$$

$$753 \quad = \int_S p_E(s) \cdot 1 ds = \int_S p_E(s) ds = 1 \quad (17)$$

755 Thus, $p_E(s, a)$ is a properly normalized joint probability density function.

756 B.3 DIFFERENCE FROM GAIL
757

758 The online learning procedure of the RAIL framework closely resembles that of GAIL, wherein a
759 discriminator is trained and its output is subsequently utilized to update the policy. However, several
760 critical distinctions differentiate RAIL from GAIL, as outlined below:

- 761 1. Unlike GAIL, RAIL introduces an additional regularization term to the discriminator objec-
762 tive function (eq. (3)).
- 763 2. GAIL employs TRPO (Schulman et al., 2015) to update the policy using the discriminator
764 output, whereas RAIL adopts a weighted BC approach for policy updates that enables the
765 online agent to stably adapt to the online environment.
- 766 3. In GAIL, action sampling is guided by online exploration to discover improved actions
767 (Ablett et al., 2023). In contrast, RAIL forgoes exploration and instead relies solely on the
768 self-supervised learning signal derived from the current action.
- 769 4. In summary, the differences between RAIL and GAIL are not limited to the discriminator
770 training process; they also reflect differing algorithmic suitability depending on the task
771 setting. GAIL is better aligned with scenarios that benefit from online exploration, whereas
772 RAIL is more suitable for settings requiring online adaptation.

773 C EXPERIMENTAL DETAILS
774775 C.1 D4RL DATASET
776

777 In this paper, we utilized D4RL dataset (Fu et al., 2021) ([https://github.com/Farama-
778 Foundation/D4RL](https://github.com/Farama-Foundation/D4RL)) for constructing expert and supplementary demonstrations. Moreover, in order to
779 ensure consistent and comparable evaluation across different environments, we report performance
780 using the standardized D4RL score metric in the overall evaluation. The D4RL score is computed as
781

$$782 \text{D4RL Score} = 100 \times \frac{R_{\text{agent}} - R_{\text{random}}}{R_{\text{expert}} - R_{\text{random}}} \quad (18)$$

783 where R_{agent} denotes the average return obtained by the evaluated policy, R_{expert} is the average return
784 of a reference expert policy, and R_{random} is the average return of a random policy defined by the D4RL
785 datasets. This normalization ensures that a score of 0 corresponds to the performance of a random
786 policy, while a score of 100 reflects expert-level performance. The resulting metric enables direct
787 comparison of policy effectiveness across different tasks and datasets.

788 C.2 IMPACT OF SUPPLEMENTARY DEMONSTRATION COVERAGE
789

790 Our ablation results of RAIL in Table 2 and Table 3 suggest that the coverage of supplementary
791 demonstrations plays a critical role in determining the success and robustness of adaptation, partic-
792 ularly under increasing noise levels. When the coverage is insufficient, the proposed method may
793 not function as intended, highlighting a potential limitation. Nevertheless, we emphasize that the
794 type of supplementary demonstrations employed in our framework can be obtained with minimal
795 effort. Such data can be automatically collected during agent training in simulation, or acquired
796 from humans, including novice users, who are relatively easy to recruit. Hence, we consider the
797 assumption of readily available supplementary demonstrations to be reasonable, and we formulated
798 our method accordingly. (ME: Medium-expert, M: Medium, MR: Medium-replay, R: Random)

801
802 Table 2: D4RL score with noise level 0.05.
803

804 Supplementary demo type	805 Hopper	806 Halfcheetah	807 Walker2d	808 Ant
809 ME	79.52 (± 0.7)	85.33 (± 0.7)	78.74 (± 1.2)	61.15 (± 0.3)
ME + M	82.99 (± 0.8)	86.19 (± 0.6)	81.52 (± 0.8)	64.08 (± 0.7)
ME + M + MR	84.30 (± 1.2)	88.97 (± 0.6)	84.97 (± 1.8)	66.17 (± 0.3)
ME + M + MR + R	85.30 (± 0.3)	89.27 (± 0.3)	86.19 (± 0.3)	68.20 (± 0.2)

810
811
812 Table 3: D4RL score with noise level 0.2.
813
814
815
816

Supplementary demo type	Hopper	Halfcheetah	Walker2d	Ant
ME	12.62 (± 1.2)	5.86 (± 1.2)	11.32 (± 1.2)	3.32 (± 0.9)
ME + M	44.86 (± 1.4)	27.77 (± 1.0)	34.98 (± 1.0)	11.28 (± 1.1)
ME + M + MR	55.47 (± 1.4)	33.62 (± 1.0)	41.01 (± 0.8)	22.22 (± 1.4)
ME + M + MR + R	62.19 (± 1.3)	49.57 (± 1.9)	48.60 (± 1.3)	38.68 (± 1.0)

817
818
819 C.3 EFFECTIVENESS OF REGULARIZED DISCRIMINATOR
820
821
822
823
824
825
826
827
828

We additionally evaluated that our regularization term is helpful for discriminator training and finally guarantees better performance. For this purpose, we add our regularization term to the discriminator loss function of ISWBC (Li et al., 2023), which we got inspired by for our study. Unlike the original experiment protocol in (Li et al., 2023), we leverages 10k expert demonstrations for the realistic setting, which is hard to acquire expert demonstrations. The result is plotted in Table 4, and there is no injected noise in the online environments. That is, this experiment is purely designed to evaluate the performance of the discriminator and how effectively it contributes to improving policy learning. From the results that applying the regularization term actually increases the final performance, we demonstrate that our discriminator function is helpful for leveraging supplementary demonstrations.

830
831 Table 4: Better performance of policy with discriminator regularization.
832
833
834

Algorithms	Hopper	Halfcheetah	Walker2d	Ant
ISWBC (Li et al., 2023)	82.45 (± 1.2)	81.76 (± 1.0)	73.93 (± 1.0)	66.76 (± 1.1)
RAIL (Ours)	88.03 (± 1.2)	84.92 (± 0.9)	78.36 (± 1.2)	71.37 (± 1.2)

835
836
837 C.4 LEARNING STABILITY OF RL AND IL IN ONLINE PHASE
838

To more specifically analyze the learning stability of RL(GAIL) and IL(RAIL), which is discussed in Sec. 2.1, we conduct an evaluation that focuses on online learning stability. To estimate learning stability, we applied an exponential moving average to the reward curve and then computed the L1 loss between the original return and the smoothed return for each episode, and averaged these values over all episodes. RAIL generally demonstrates superior results to those of GAIL, as in Table 5.

839
840 Table 5: Learning stability of GAIL and RAIL with $\sigma = 0.2$.
841
842
843

Algorithm	Hopper	Halfcheetah	Walker2d	Ant
GAIL (Ho & Ermon, 2016)	6.4 (± 0.3)	9.2 (± 0.1)	7.1 (± 0.3)	10.1 (± 0.2)
RAIL	3.5 (± 0.2)	5.4 (± 0.1)	4.9 (± 0.3)	14.8 (± 0.2)

844
845
846 D IMPLEMENTATION DETAILS
847
848

849 D.1 HYPERPARAMETERS

We first describe the network architecture and then the hyperparameters we used. First, for the network architecture, we build our network based on DWBC (Xu et al., 2022) (<https://github.com/ryanxhr/DWBC>) and ISWBC (Li et al., 2023) (<https://github.com/liziniu/ISWBC>). For the policy, we compose five hidden multilayer perceptron (MLP) layers with a size of 256×256 . On top of this, we completed the full network architecture of the policy by incorporating an input layer and an output layer, aligned with the dimensionalities of the state and action spaces, respectively. Next, for the discriminator, we construct the discriminator network with three hidden MLP layers with a size of 256×256 . The input to the network was designed to accept both the state and action simultaneously, while the output was a single float value in the range $[0, 1]$. To enhance training stability, the output was clipped to lie within the range $[0.01, 0.99]$. Related hyperparameters for

864 training discriminator and policy are stated in Table 6 and Table 7, respectively. t in the BC weight λ
 865 in Table 7 indicates training timesteps.
 866

867 Table 6: Hyperparameters used for discriminator.
 868

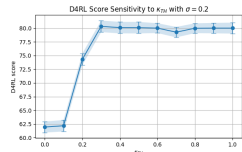
869 Hyperparameter	870 Value
871 Learning rate	5×10^{-4}
872 Batch size	64
873 Optimizer	Adam

874 Table 7: Hyperparameters used for policy.
 875

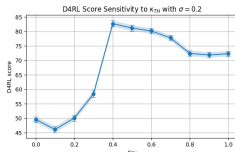
876 Hyperparameter	877 Value
878 Learning rate	5×10^{-4}
879 Batch size	64
880 Optimizer	Adam
881 Regularizer weight λ	$\lambda = \begin{cases} 1, & \text{if } t \leq 10000 \\ \frac{1}{1+\log(t-9999)}, & \text{if } t > 10000 \end{cases}$
882	20
883	

885

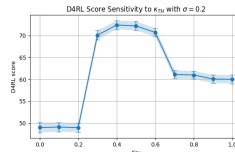
D.2 PERFORMANCE SENSITIVITY TO κ_{TH}

 886

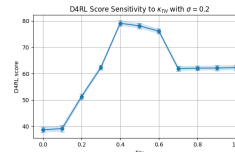
(a) Hopper



(b) Halfcheetah



(c) Walker2d



(d) Ant

895 Figure 4: Performance variation with respect to κ_{TH} .
 896

897 We determined the optimal value of κ_{TH} empirically through a grid-search procedure. Since the
 898 formulation of κ_{TH} constrains it to lie within the interval $[0, 1]$, we evaluated performance at
 899 increments of 0.1, and the results are shown in Fig. 4. A smaller value of κ_{TH} indicates that
 900 online learning is rarely triggered, whereas a larger value implies that online learning occurs at
 901 many timesteps. From these results, we observe that setting $\kappa_{TH} = 0.4$ yields the highest overall
 902 performance. This corresponds to cases where $p_E(s)$ or $p_S(s)$ lies within the range 0.8–1.0, indicating
 903 a high likelihood that the sampled state belongs to the offline dataset. Based on this observation, we
 904 set the threshold to $\kappa_{TH} = 0.4$ for all subsequent experiments.
 905

906

E THE USE OF LARGE LANGUAGE MODELS (LLMs)

 907

908 In this paper, assistance from large language models (LLMs) was limited solely to the writing process,
 909 such as grammar and phrasing.
 910

911

F LIMITATIONS

 912

913 A limitation of our method lies in the assumption that supplementary demonstrations visit states that
 914 are not covered by expert demonstrations, which implies no overlap. While this assumption is looser
 915 than that of prior works (Li et al., 2023), which require the expert’s stationary state-action distribution
 916 to fully cover the domain, our approach may not be applicable in environments where trajectories are
 917 constrained to a limited set of states. Furthermore, accurate PDF approximation and probability-based
 918 regularization rely on the supplementary demonstrations visiting the non-expert states in a sufficiently

918 uniform manner. For future work, our approach may be extended by incorporating techniques for
919 obtaining an unbiased PDF from biased demonstrations.
920
921
922
923
924
925
926
927
928
929
930
931
932
933
934
935
936
937
938
939
940
941
942
943
944
945
946
947
948
949
950
951
952
953
954
955
956
957
958
959
960
961
962
963
964
965
966
967
968
969
970
971